APPENDIX 4A BODE PLOTS OF TRANSFER FUNCTIONS WITH POLES AND ZEROS

In this section, Bode plots of various transfer functions are presented as a review.

4A-1 A Pole in a Transfer Function

A transfer function with a pole at ω_p is expressed below

$$T(s) = \frac{1}{1 + \dfrac{s}{\omega_p}} \tag{4A-1}$$

whose gain and phase plots in Fig. 4A-1 show that the gain beyond the pole frequency of ω_p starts to fall at a rate of –20 dB/decade and the phase angle falls to -90^0 approximately a decade later.

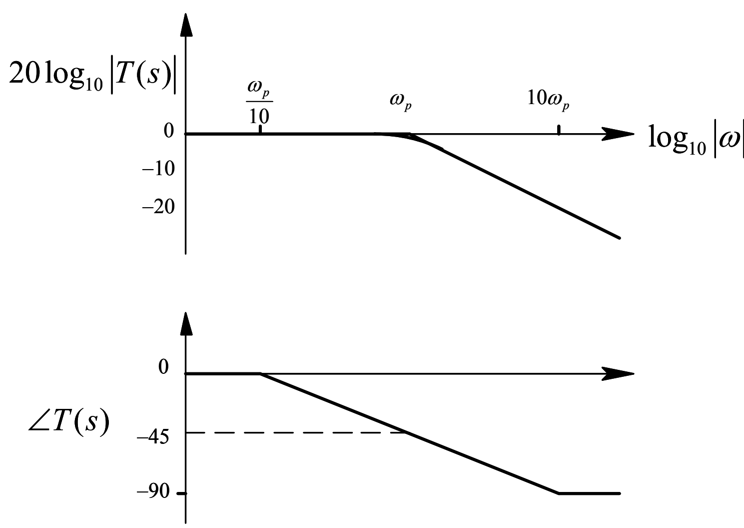

Fig. 4A-1 Gain and phase plots of a pole.

4A-2 A Zero in a Transfer Function

The transfer function with a zero at a frequency of ω_z is expressed below

$$T(s) = 1 + \frac{s}{\omega_z} \tag{4A-2}$$

whose gain and phase plots in Fig. 4A-2 show that the gain beyond the frequency of ω_z starts to rise at a rate of 20 *dB/decade* and the phase angle rises to $+90^0$ approximately a decade later.

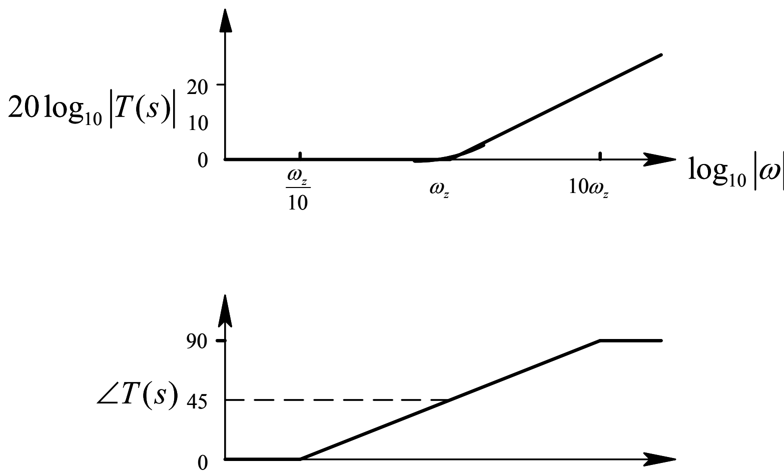

Fig. 4A-2 Gain and phase plots of a zero.

4A-3 A Right-Hand-Plane (RHP) Zero in a Transfer Function

In boost and buck-boost dc-dc converters, transfer functions contain a so called right-hand plane (RHP) zero, with a transfer function expressed below

$$T(s) = 1 - \frac{s}{\omega_z} \tag{4A-3}$$

whose gain and phase plots in Fig. 4A-3 show that the gain beyond the frequency of ω_z starts to rise at a rate of 20 *dB/decade* while the phase angle drops to -90^0 approximately a decade later. This RHP zero presents special challenges in designing feedback controllers in boost and buck-boost converters, as is discussed in this chapter.

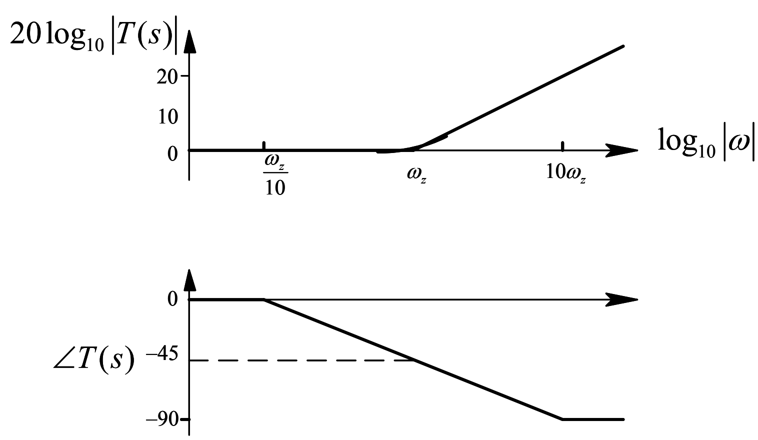

Fig. 4A-3 Gain and phase plots of a right-hand side zero.

Appendix 4-2

4A-4 A Double Pole in a Transfer Function

In dc-dc converter transfer functions, presence of L-C filters introduces a double pole, that can be expressed as below

$$T(s) = \frac{1}{1 + \alpha s + \left(\frac{s}{\omega_o}\right)^2} \tag{4A-4}$$

whose gain and plots in Fig. 4A-4 show that the gain beyond the frequency ω_o starts to fall at a rate of –40 *dB/decade* and the phase angle falls towards -180^0. These plots depend on the damping coefficient $\xi = (\alpha/2)\omega_o$.

APPENDIX 4B TRANSFER FUNCTIONS IN CONTINUOUS CONDUCTION MODE (CCM)

In this section, we will derive the transfer function $\tilde{v}_o/\tilde{d}$ for the three converters operating in CCM

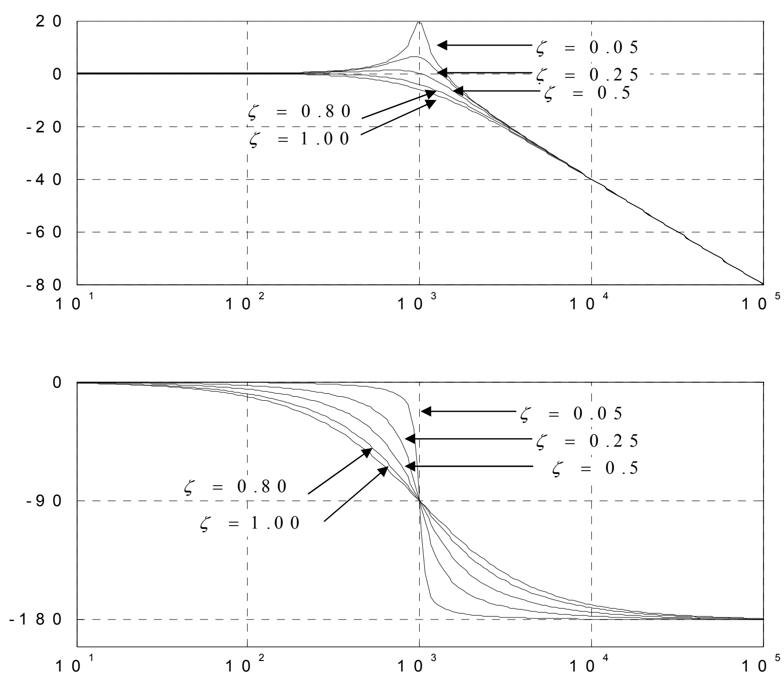

Fig.4A-4 Gain and phase plots of a double-pole.

4B-1 Buck Converters

From Fig. 4-7, the small signal diagram for a Buck converter is shown in Fig. 4B-1. Defining the output stage impedance Z_{os} as the parallel combination of the filter capacitor and the load resistance,

$$Z_{os} = \frac{R(r+\frac{1}{sC})}{R+(r+\frac{1}{sC})} = R\frac{1+srC}{1+s(R+r)C} \tag{4B-1}$$

In any practical converter, $r \ll R$, and therefore, $R+r \simeq R$. Making use of this assumption in Eq. 4B-1,

$$Z_{os} \simeq R\frac{1+srC}{1+sRC} \tag{4B-2}$$

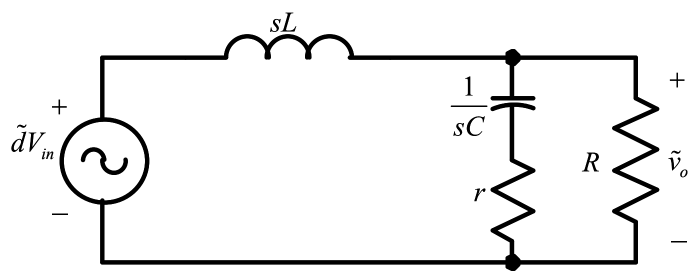

Fig. 4B-1 Equivalent circuit of average buck converter.

Defining Z_{eff} as the sum of the filter inductor and the output stage impedance,

$$Z_{eff} = sL + Z_{os} = \frac{1+srC}{LC\left[s^2+s\left(\frac{1}{RC}+\frac{r}{L}\right)+\frac{1}{LC}\right]} \tag{4B-3}$$

Therefore, in the Fig. 4B-1 by voltage division

$$\frac{\tilde{v}_o}{\tilde{d}} = V_{in}\frac{Z_{os}}{Z_{eff}} = V_{in}\frac{1+srC}{LC\left[s^2+s\left(\frac{1}{RC}+\frac{r}{L}\right)+\frac{1}{LC}\right]} \tag{4B-4}$$

4B-2 Boost Converter

From Fig. 4-7, the small signal diagram of a Boost converter is shown in Fig. 4B-2a. In this circuit, the dc steady state operating point values can be calculated as follows:

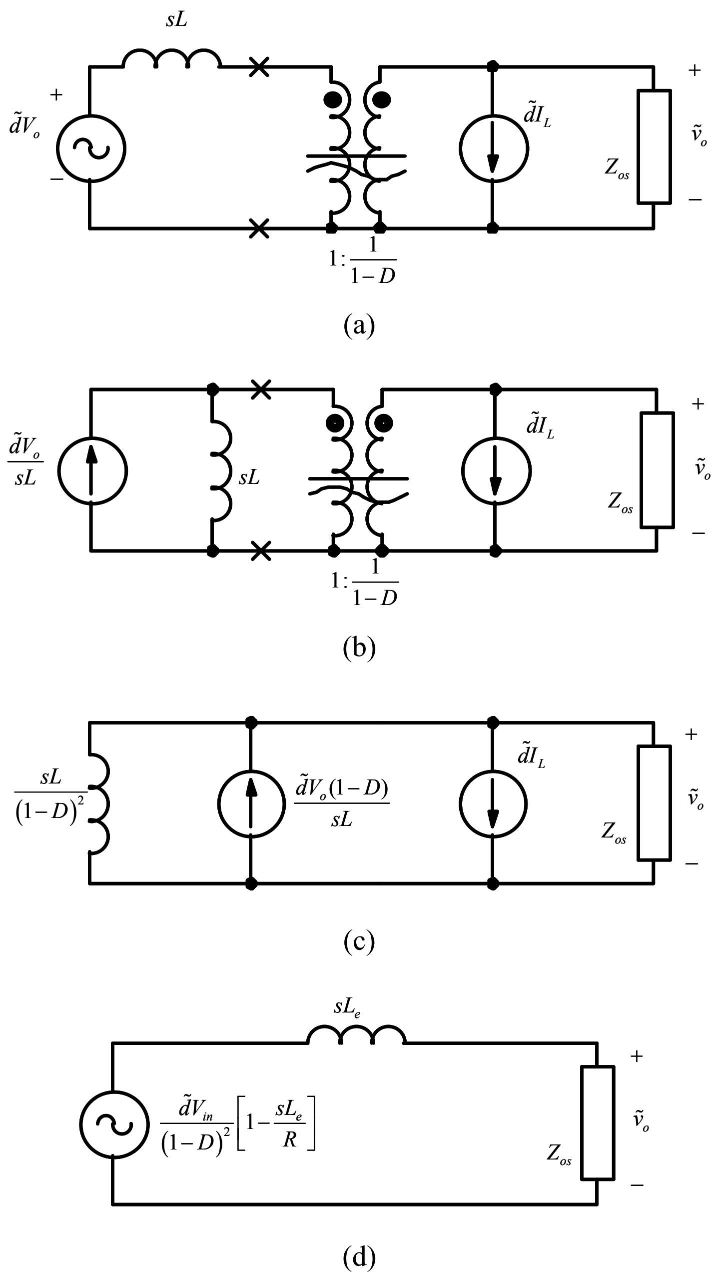

Fig. 4B-2 Equivalent circuit of average boost converter.

$$I_o = \frac{V_o}{R} \tag{4B-5}$$

Equating the input and the output power,

$$V_o I_o = V_{in} I_{in} \tag{4B-6}$$

Substituting Eq. 4B-5 into Eq. 4B-6,

$$I_L = I_{in} = \frac{V_o I_o}{V_{in}} = \frac{V_o^2}{RV_{in}} \tag{4B-7}$$

In Fig. 4B-2a, the sub-circuit left of the marked terminals can be replaced by its Norton equivalent, as shown in Fig. Fig. 4B-2b. The sub-circuit left of the transformer in FIg. 4B-2b can be transformed to the right, as shown in Fig. 4B-2c, where

$$L_e = \frac{L}{(1-D)^2} \tag{4B-8}$$

The two current sources in Fig. 4B-2c can be combined and using the Thevenin's equivalent, the equivalent voltage in Fig. 4B-2d is

$$v_{eq} = \tilde{d}\frac{V_{in}}{(1-D)^2}\left(1-\frac{sL_e}{R}\right) \tag{4B-9}$$

Using the equivalent voltage in Eq. 4B-9 and applying the voltage division in the circuit of Fig. 4B-2d,

$$\frac{\tilde{v}_o}{\tilde{d}} = \frac{V_{in}}{(1-D)^2}\left(1-\frac{sL_e}{R}\right)\frac{1+srC}{L_eC\left[s^2+s\left(\frac{1}{RC}+\frac{r}{L_e}\right)+\frac{1}{L_eC}\right]} \tag{4B-10}$$

4B-3 Buck-Boost Converter

From Fig. 4-7, the small signal diagram of a Buck-Boost converter is shown in Fig. 4B-3a. First, we will calculate the values of the needed quantities at the dc steady state operating point.

In a Buck-Boost converter,

$$I_o = \frac{V_o}{R} \tag{4B-11}$$

$$V_o = \frac{D}{1-D}V_{in} \tag{4B-12}$$

Equating the input and the output power,

$$I_{in}V_{in} = V_o I_o \tag{4B-13}$$

and hence,

$$I_{in} = \frac{V_o^2}{RV_{in}} \tag{4B-14}$$

Since, $I_L = I_o + I_{in}$,

$$I_L = \frac{V_{in}}{R}\frac{D}{\left(1-D\right)^2} \tag{4B-15}$$

Considering the sub-circuit to the left of the marked terminals in Fig. 4B-3a and drawn in Fig. 4B-3b,

$$i_1 = i_2 \tag{4B-16}$$

where,

$$i_1 = Di_2 \tag{4B-17}$$

Eqs. 4B-16 and 4B-17 are valid in general only if $i_1 = i_2 = 0$. Therefore in Fig. 4B-3b,

$$v_{oc} = \tilde{d}\frac{V_{in}}{\left(1-D\right)^2} \tag{4B-18}$$

Shorting the terminals as shown in Fig. 4B-3c,

$$i_{sc} = i_1 - Di_1 = \left(1-D\right)i_1 \tag{4B-19}$$

In Fig. 4B-3c,

$$i_1 = \tilde{d}\frac{V_{in}}{\left(1-D\right)sL} \tag{4B-20}$$

Substituting Eq. 4B-20 into Eq. 4B-19,

$$i_{sc} = \tilde{d}\frac{V_{in}}{sL} \tag{4B-21}$$

From Figs. 4B-3b and 4B-3c, and Eqs. 4B-18 and 4B-21, the Thevenin impedance to the left of the marked terminals in Fig. 4B-3a is

$$Z_{Th} = \frac{v_{oc}}{i_{sc}} = sL_e \tag{4B-22}$$

where

$$L_e = \frac{L}{\left(1-D\right)^2} \tag{4B-23}$$

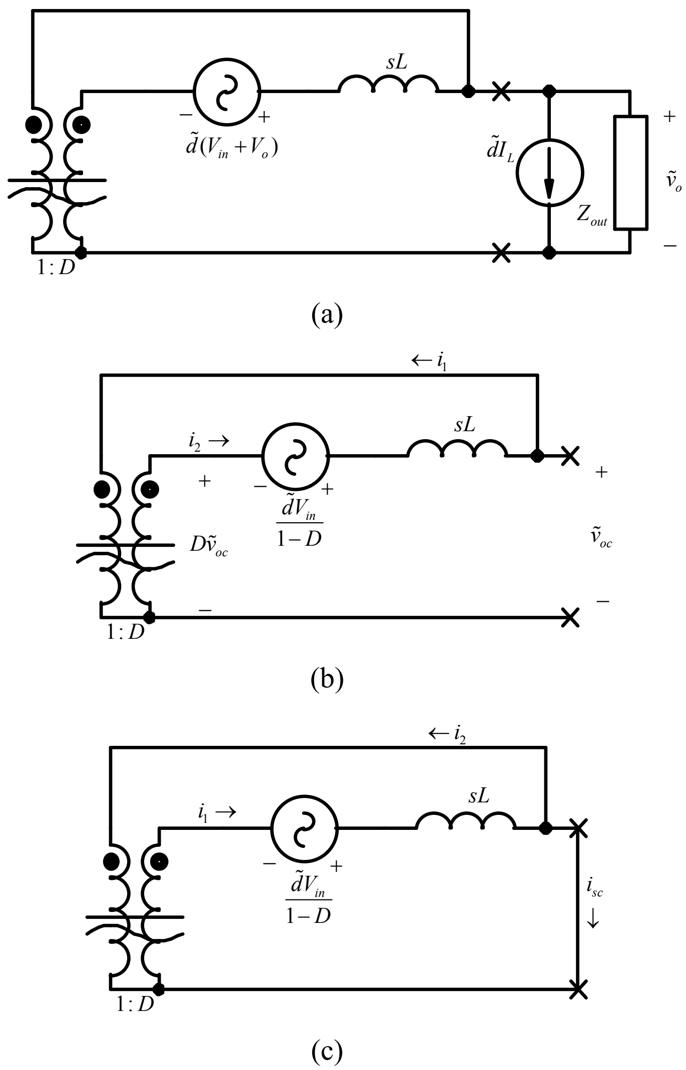

Fig. 4B-3 Equivalent circuit of average buck-boost converter.

and,

$$v_{Th} = \tilde{d}\frac{V_{in}}{\left(1-D\right)^2} \tag{4B-24}$$

With this Thevenin equivalent, the circuit of Fig. 4B-3a, can be drawn as shown in Fig. 4B-4a. The sub-circuit to the left of the marked terminals can be represented by its Norton equivalent, as shown in Fig. 4B-4b. Combining the current sources and representing the sub-circuit in Fig. 4B-4b by its Thevenin equivalent as shown in Fig. 4B-4c,

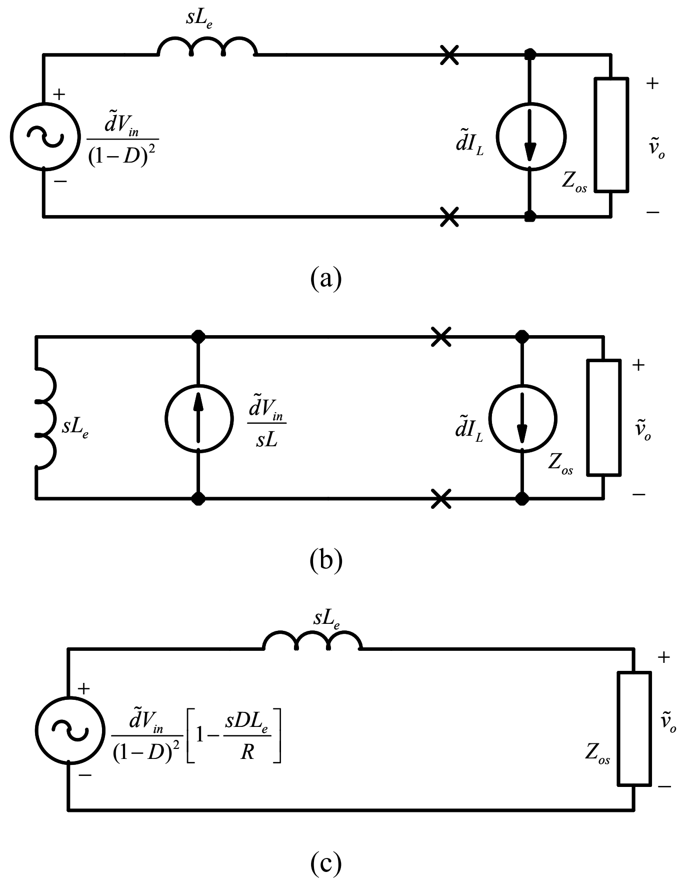

Fig. 4B-4 Equivalent circuit of average buck-boost converter (contd.)

$$v_{eq} = \tilde{d}\,\frac{V_{in}}{(1-D)^2}\left(1 - sD\frac{L_e}{R}\right) \tag{4B-25}$$

Hence,

$$\frac{\tilde{v}_o}{\tilde{d}} = \frac{V_{in}}{(1-D)^2}\left(1 - sD\frac{L_e}{R}\right)\frac{1 + srC}{L_eC\left[s^2 + s\left(\frac{1}{RC} + \frac{r}{L_e}\right) + \frac{1}{L_eC}\right]} \tag{4B-26}$$

APPENDIX 4C DERIVATION OF PARAMETERS OF THE CONTROLLER TRANSFER FUNCTIONS

4C-1 CONTROLLER TRANSFER FUNCTION WITH ONE POLE-ZERO PAIR

$$G_c(s) = k_c \frac{1 + s/\omega_z}{1 + s/\omega_p} \tag{4C-1}$$

$$\phi = \angle G_c(s) = \tan^{-1}\frac{\omega}{\omega_z} - \tan^{-1}\frac{\omega}{\omega_p} \tag{4C-2}$$

4C-1-1 Frequency at which ϕ_{boost} Occurs

The maximum angle ϕ_{boost} provided by the controller occurs at the geometric mean of the zero and pole frequencies, as shown below. (This geometric mean frequency is made to coincide with $\omega = \omega_c$ where ω_c is the cross over frequency.) To find the frequency at which ϕ_{boost} occurs, we will set the derivative of the phase angle to zero:

$$\frac{d}{d\omega}\phi = \frac{1}{\omega_z}\frac{1}{\left(1+\dfrac{\omega^2}{\omega_z^{\,2}}\right)} - \frac{1}{\omega_p}\frac{1}{\left(1+\dfrac{\omega^2}{\omega_p^{\,2}}\right)} = 0 \tag{4C-3}$$

Therefore,

$$\frac{\omega_z}{\left(\omega^2 + \omega_z^{\,2}\right)} - \frac{\omega_p}{\left(\omega^2 + \omega_p^{\,2}\right)} = 0 \tag{4C-4}$$

or,

$$\left(\omega^2 - \omega_z\omega_p\right)\left(\omega_z - \omega_p\right) = 0 \tag{4C-5}$$

From Eq. 4C-5,

$$\omega = \sqrt{\omega_z\omega_p} \tag{4C-6}$$

which shows that the phase angle of the controller transfer function reaches its maximum at the geometric-mean frequency.

4C-1-2 Deriving the Zero and Pole Frequencies

Substituting Eq. 4C-4 into Eq. 4C-2,

$$\phi_{boost} = \tan^{-1}\frac{\sqrt{\omega_z \omega_p}}{\omega_z} - \tan^{-1}\frac{\sqrt{\omega_z \omega_p}}{\omega_p} \tag{4C-7}$$

or,

$$\phi_{boost} = \tan^{-1}\sqrt{\frac{\omega_p}{\omega_z}} - \tan^{-1}\sqrt{\frac{\omega_z}{\omega_p}} \tag{4C-8}$$

Note that $\tan^{-1} x = \cot^{-1}\left(\frac{1}{x}\right)$ and $\tan^{-1} y + \cot^{-1} y = \frac{\pi}{2}$. Therefore, in Eq. 4C-8

$$\phi_{boost} = \tan^{-1}\sqrt{\frac{\omega_p}{\omega_z}} - \left(\frac{\pi}{2} - \tan^{-1}\sqrt{\frac{\omega_p}{\omega_z}}\right) = 2\tan^{-1}\sqrt{\frac{\omega_p}{\omega_z}} - \frac{\pi}{2} \tag{4C-9}$$

We will define an intermediate variable, called the K-factor, as

$$K_{boost} = \sqrt{\frac{\omega_p}{\omega_z}} \tag{4C-10}$$

Solving Eqs. 4C-9 and 4C-10

$$K_{boost} = \tan\left(\frac{\phi_{boost}}{2} + \frac{\pi}{2}\right) \tag{4C-11}$$

or,

$$K_{boost} = \tan\left(\frac{\phi_{boost}}{2} + 45^\circ\right) \tag{4C-12}$$

4C-1-2 Realizing the Controller Transfer Function with a Single Op-Amp

The controller transfer function in Eq. 4C-1 can be realized by a single op-amp, as derived below.

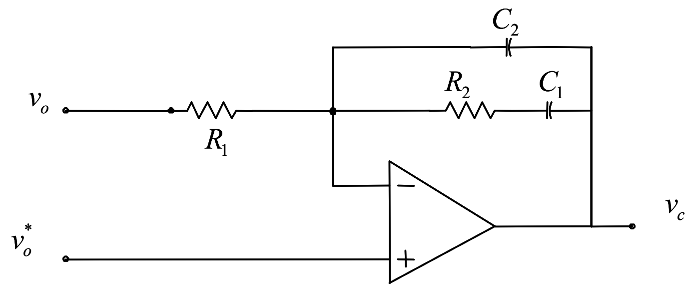

Figure 4C-1 Implementation of the controller transfer function in Eq. 4C-1.

In Fig. 4C-1, we can derive that

$$k_c = \frac{1}{R_1(C_1 + C_2)}$$
$$\omega_z = \frac{1}{C_1 R_2} \qquad \text{(4C-13)}$$
$$\omega_p = \frac{C_1 + C_2}{R_2 C_1 C_2}$$

From Eq. 4C-13, in terms of R_1

$$C_2 = \frac{\omega_z}{\omega_p R_1 k_c}$$
$$C_1 = C_2(\omega_p / \omega_z - 1) \qquad \text{(4C-14)}$$
$$R_2 = 1/(\omega_z C_1)$$

4C-2 CONTROLLER TRANSFER FUNCTION WITH TWO POLE-ZERO PAIRS

A similar derivation can be carried out where,

$$G_c(s) = k_c \frac{(1 + s/\omega_z)^2}{(1 + s/\omega_p)^2} \qquad \text{(4C-15)}$$